

1 **Sex-specific co-expression networks and sex-biased gene expression in the**
2 **salmonid Brook Charr *Salvelinus fontinalis***

3 Ben J. G. Sutherland^{1†*}, Jenni M. Prokkola², Céline Audet³, and Louis Bernatchez¹

4 ¹ Institut de Biologie Intégrative et des Systèmes (IBIS), Université Laval, Québec, QC G1V 0A6, Canada

5 ² Institute of Integrative Biology, University of Liverpool, L69 7ZB Liverpool, UK

6 ³ Institut des Sciences de la Mer de Rimouski, Université du Québec à Rimouski, Rimouski, QC G5L
7 3A1, Canada

8 †Current Address: Pacific Biological Station, Fisheries and Oceans Canada, Nanaimo, BC, V9T 6N7,
9 Canada

10

11 *Author for correspondence: BJGS

12 Pacific Biological Station, Fisheries and Oceans Canada, Nanaimo, BC, Canada

13 Phone: 1 (250) 751-4676

14 Email: ben.sutherland.1@ulaval.ca (BS)

15

16

17

18 **Data Deposition:** Brook Charr raw sequence data has been uploaded to SRA under BioProject

19 PRJNA445826, accession SRP136537. Arctic Charr raw sequence data is available under BioProject

20 PRJNA307980, accession SRP068854.

ABSTRACT

21
22 Networks of co-expressed genes produce complex phenotypes associated with functional novelty. Sex
23 differences in gene expression levels or in the structure of gene co-expression networks can cause sexual
24 dimorphism and may resolve sexually antagonistic selection. Here we used RNA-sequencing in the
25 salmonid Brook Charr *Salvelinus fontinalis* to characterize sex-specific co-expression networks in the
26 liver of 47 female and 53 male offspring. In both networks, modules were characterized for functional
27 enrichment, hub gene identification, and associations with 15 growth, reproduction, and stress-related
28 phenotypes. Modules were then evaluated for preservation in the opposite sex, and in the congener Arctic
29 Charr *Salvelinus alpinus*. Overall, more transcripts were assigned to a module in the female network than
30 in the male network, which coincided with higher inter-individual gene expression and phenotype
31 variation in the females. Most modules were preserved between sexes and species, including those
32 involved in conserved cellular processes (e.g. translation, immune pathways). However, two sex-specific
33 male modules were identified, and these may contribute to sexual dimorphism. To compare with the
34 network analysis, differentially expressed transcripts were identified between the sexes, revealing a total
35 of 16% of expressed transcripts as sex-biased. For both sexes, there was no overrepresentation of sex-
36 biased genes or sex-specific modules on the putative sex chromosome. Sex-biased transcripts were also
37 not overrepresented in sex-specific modules, and in fact highly male-biased transcripts were enriched in
38 preserved modules. Comparative network analysis and differential expression analyses identified different
39 aspects of sex differences in gene expression, and both provided new insights on the genes underlying
40 sexual dimorphism in the salmonid Brook Charr.

41
42
43
44
45
46
47
48 **Keywords:** Co-expression; Salmonid; Sex-bias; Sexual Dimorphism; Transcriptomics; Weighted Gene
49 Co-expression Network Analysis (WGCNA)

51

INTRODUCTION

52 Understanding how sex bias in gene expression contributes to sexually dimorphic phenotypes, and how
53 this affects fitness is an important area of study to understand genotype-phenotype interactions (Parsch
54 and Ellegren 2013). The development of sex differences in phenotypes can be attributed to differences in
55 the expression of both sex-specific and autosomal genes, caused by hormonal and epigenetic effects
56 (Ellegren and Parsch 2007; Wijchers and Festenstein 2011), heterogamy and imperfect dosage
57 compensation (Parsch and Ellegren 2013), epistatic interactions, and transcriptional network structural
58 differences (Chen *et al.* 2016). Sex-biased gene expression is pervasive in many species and may alleviate
59 sexually antagonistic selection, i.e., the selection for different phenotypes in the different sexes (Wright *et*
60 *al.* 2018; Rowe *et al.* 2018). Transcriptome regulatory architecture differences between the sexes may
61 contribute to the development of sex-biased gene expression (Chen *et al.* 2016; Wright *et al.* 2018). Sex-
62 biased expression underlies much of phenotypic sexual dimorphism, which can occur without sexually
63 antagonistic selection (e.g. imperfect dosage compensation; Parsch and Ellegren 2013). To connect alleles
64 to phenotypes, typically association studies are applied (Mackay, 2001; Bush and Moore 2012), but these
65 bypass important intermediate regulatory steps such as transcriptome regulation (Mackay *et al.* 2009). To
66 characterize transcriptome regulation, it is important to consider the underlying structure of the network
67 in which genes are co-regulated (Mähler *et al.* 2017).

68 Constructing gene co-expression networks is often based on correlating transcript abundance
69 across samples (Langfelder and Horvath 2008). A network is comprised of modules, each of which is
70 comprised of a group of genes with correlated expression patterns. Co-expression clustering is a valuable
71 approach to classify and visualize transcriptomic data (Eisen *et al.* 1998). Clustering often groups genes
72 together that have similar cellular functions and regulatory pathways (Eisen *et al.* 1998), although this is
73 not always the case (Gillis and Pavlidis 2012; van Dam *et al.* 2017). Module functions can be predicted
74 based on phenotypic correlations (Filteau *et al.* 2013; Rose *et al.* 2015) or functional enrichment analysis
75 (e.g. Gene Ontology). Genes that are highly connected and central to a module (i.e., hub genes) may be
76 upstream regulators of the module, and potentially more related to the module function (van Dam *et al.*
77 2017). Hub genes may also be under higher selective constraint than other less connected genes, and as a
78 result may show lower genetic variation and higher phylogenetic conservation (Mähler *et al.* 2017).
79 Network information thus provides novel insight into both gene activity and evolution.

80 Comparative network analysis across species can advance the understanding of species-specific
81 innovations. For example, comparing brain transcriptome networks between chimpanzee *Pan troglodytes*
82 and human *Homo sapiens* indicates low preservation of modules found in specific brain regions
83 associated with human evolution such as the cerebral cortex (Oldham *et al.* 2006). Comparing networks
84 can highlight potential drivers of phenotypic changes associated with adaptive divergence that can lead to

85 ecological speciation (Filteau *et al.* 2013; Thompson *et al.* 2015). Cross-species network comparisons
86 have also been used to detect gene modules associated with disease (Mueller *et al.* 2017) or with seasonal
87 phenotypic changes (Cheviron and Swanson 2017). These insights are often not possible to obtain
88 through standard gene-by-gene differential expression analysis, which captures a smaller proportion of
89 the variation than differential co-expression analysis (Oldham *et al.* 2006; Gaiteri *et al.* 2014).

90 Network comparisons can also provide insight on sex differences (Chen *et al.* 2016). Differing
91 structure of networks between the sexes may resolve sexual antagonism through gene regulation (Chen *et*
92 *al.* 2016). Other genetic architecture solutions to this conflict may include sex-dependent dominance
93 (Barson *et al.* 2015) or maintaining alleles associated with sexual antagonism on sex chromosomes
94 (Blackmon and Brandvain 2017). Comparisons between the sexes are complicated by the fact that sex
95 bias in networks can be tissue-specific, with modules more preserved between sexes in brain and muscle
96 networks than in liver or adipose tissue (van Nas *et al.* 2009; Wong *et al.* 2014). Liver tissue is considered
97 a highly sexually dimorphic tissue, particularly in oviparous species at a reproductive stage (Qiao *et al.*
98 2016). Although the extent of differences may depend on the tissue of study, network comparisons
99 between sexes can provide new insight into the regulatory underpinnings of sexual dimorphism and
100 antagonism.

101 Salmonids are an important species of commercial, ecological, and cultural value. This species
102 group is also a model system for studying genome evolution after a whole genome duplication event that
103 occurred approx. 80-100 million years ago (Allendorf and Thorgaard 1984; Crête-Lafrenière *et al.* 2012;
104 Macqueen and Johnston 2014). Charr (*Salvelinus* spp.) are a phenotypically diverse group of salmonids
105 that are less characterized in terms of transcriptomic and genomic data than other genera (e.g. *Salmo* or
106 *Oncorhynchus*; but see Carruthers *et al.* 2018; Christensen *et al.* 2018; Guðbrandsson *et al.* 2018). Brook
107 Charr *S. fontinalis* is a primarily freshwater species native to Eastern North America. Arctic Charr *S.*
108 *alpinus* has a circumpolar distribution mainly in the Arctic, and these two lineages diverged
109 approximately 10 million years ago (Horreo 2017). Sexual dimorphism in body size and secondary sexual
110 characteristics is associated with reproductive success in Brook Charr and other salmonids (Quinn and
111 Foote 1994). The largest males are typically dominant and fertilize the majority of a brood (Blanchfield *et*
112 *al.* 2003), but smaller sneaker males can also contribute in fertilization. In females however, large body
113 size is more constrained as it is highly associated to fecundity, and smaller life history variants are not
114 expected (reviewed by Fleming 1998). With different optimal reproductive-associated phenotypes
115 between the sexes, this could give rise to sexual dimorphism as well as sexual antagonism.

116 Here we profile liver transcriptomes of 100 Brook Charr offspring from a single family by RNA-
117 sequencing to characterize co-expression patterns. Transcriptome profiling was conducted shortly (3 h)
118 after the application of an acute handling stressor to all individuals during the reproductive season,

119 increasing variance among individuals. The goals of this study are to i) characterize the sex-specific or
120 preserved modular structure of gene co-expression in liver tissue in Brook Charr; ii) characterize module
121 preservation in the congener Arctic Charr to investigate evolutionary conservation of the networks; iii)
122 connect phenotype and functional category associations to the identified modules; and iv) integrate results
123 from the network analyses with a gene-by-gene differential expression analysis to determine whether the
124 two methods provide different insights on sexual dimorphism in transcriptome architecture.

125

126

MATERIALS AND METHODS

Animals and sample collection

128 Brook Charr used in this study were originally used to construct a low-density genetic map for
129 reproductive (Sauvage *et al.* 2012a), growth and stress response QTL analyses (Sauvage *et al.* 2012b).
130 They were used to construct a high-density genetic map that was integrated with the other salmonids
131 (Sutherland *et al.* 2016), then used to identify QTL, sex-specific recombination rates, and the Brook Charr
132 sex chromosome (Sutherland *et al.* 2017). The 192 F₂ individuals were full sibs from a single family
133 resulting from a cross of an F₁ female and F₁ male that were from an F₀ female from a wild anadromous
134 population (Laval River, near Forestville, Québec) and an F₀ male from a domestic population (Québec
135 aquaculture over 100 years).

136 F₂ offspring were raised until 65-80 g and then 21 phenotypes were collected along with several
137 repeat measurements to determine growth rate. Full details on these phenotypes are previously described
138 (Sauvage *et al.* 2012a, 2012b), including sex-specific phenotype averages, standard deviations, and
139 phenotype correlations for all 192 offspring (see Table S1 and Figure S2 from Sutherland *et al.* 2017).
140 The 15 phenotypes used in the present study to correlate with co-expression modules were maturity,
141 length, weight, growth rate, condition factor, liver weight, post-stress cortisol, osmolality and chloride,
142 change in cortisol, osmolality and chloride between one week before and three hours after an acute
143 handling stress, egg diameter, sperm concentration, and sperm diameter. Fish were anaesthetized with 3-
144 aminobenzoic acid ethyl ester and killed by decapitation as per regulations of Canadian Council of
145 Animal Protection recommendations approved by the University Animal Care Committee, as previously
146 reported (Sauvage *et al.* 2012a). A total of 87% of the 47 females and 96% of the 53 males used for
147 transcriptome profiling were in a reproductive state at the time of the dissection, which was in the fall
148 (smolting occurs in this strain in the spring; Boula *et al.* 2002). Phenotypic sex was determined by gonad
149 inspection (Sauvage *et al.* 2012b). Immediately after decapitation, liver tissue was excised, flash frozen
150 then kept at -80 °C until RNA extraction.

151

152 *RNA extraction and library preparation*

153 A total of 100 of the 192 individuals were used for liver transcriptome profiling. Prior to extraction,
154 samples were assigned random order to reduce batch effects on any specific group of samples. Total RNA
155 was extracted from equal sized pieces of liver tissue from approximately the same location on the liver for
156 all samples (0.4 x 0.2 x 0.2 cm; ~1 mg). This piece was rapidly immersed in 1 ml TRIzol (Invitrogen),
157 then placed on dry ice until all samples per batch were prepared (6-12 per extraction round). When all
158 samples were ready, the samples immersed in frozen TRIzol were allowed to slightly thaw for
159 approximately 1 min until beads within the vials were able to move, then the samples were homogenized
160 for 3 min at 20 hz, rotated 180°, and homogenized again for 3 min at 20 hz on a MixerMill (Retsch). The
161 homogenate was centrifuged at 12,000 x g for 10 min at 4 °C. The supernatant was transferred to a new 2
162 ml tube and incubated for 5 min at room temperature. Chloroform (200 µl) was added to the tube, the tube
163 was shaken vigorously for 15 s and incubated 3 min at room temperature, then centrifuged at 12,000 x g
164 for 15 min at 4 °C. Finally the aqueous layer was carefully transferred to a new centrifuge tube, and into
165 an RNeasy spin column (QIAGEN), as per manufacturer's instructions with the optional on-column
166 DNase treatment. All samples were quality checked using a BioAnalyzer (Agilent), where all samples had
167 RIN ≥ 8.3 (mean = 9.5), and were quantified using spectrophotometry on a Nanodrop-2000 (Thermo
168 Scientific).

169 Libraries were prepared using 1 µg of total RNA in the randomized order using TruSeq RNA
170 Sample Prep Kit v2 (Illumina) to generate cDNA as per manufacturer's instructions using adapters from
171 both Box A and Box B, AMPure XP beads (Agencourt) and a magnetic plate in batches of 8-16 samples
172 per batch. Fragmentation times of 2, 4 and 6 min were tested for optimal size fragmentation and
173 consistency, and as a result of this test, all samples were processed using a 6 min fragmentation time.
174 PCR amplification to enrich cDNA was performed using 15 cycles, as per manufacturer's instructions.
175 All libraries were quantified using Quant-iT PicoGreen (ThermoFisher) and quality-checked using the
176 BioAnalyzer on High Sensitivity chips (Agilent) for consistent size profiles. Once all samples were
177 confirmed to be high quality and of approximately the same insert size, eight individually tagged samples
178 were pooled in equimolar quantities (80 ng per sample) and sent to McGill Sequencing Center for 100 bp
179 single-end sequencing on a HiSeq2000 (Illumina; total = 13 lanes). Parents (F₁ individuals) were
180 sequenced in duplicate in two separate lanes.

181

182 *RNA-seq mapping*

183 Quality trimming and adapter removal was performed using Trimmomatic (Bolger et al. 2014), removing
184 adapters with the *-illuminaclip* (2:30:10) option and removing low quality reads (< Q2) using *-*
185 *slidingwindow* (20:2), *-leading* and *-trailing* options. Q2 was used for optimal quantification as previously

186 demonstrated (MacManes 2014). A reference transcriptome for Brook Charr was obtained from the
187 Phylofish database (Pasquier *et al.* 2016). Trimmed reads were mapped against the reference
188 transcriptome with *bowtie2* (Langmead and Salzberg 2012) using *--end-to-end* mode reporting multiple
189 alignments (*-k* 40) for optimal use with eXpress for read count generation (Roberts and Pachter 2013).
190 The multiple alignment file was converted to bam format and sorted by read name using SAMtools (Li *et*
191 *al.* 2009) and input to eXpress (see full bioinformatics pipeline in *Data Availability*).

192 Read counts were imported into edgeR (Robinson *et al.* 2010) for normalization and low
193 expression filtering. The smallest library (lib87, 8,373,387 aligned reads) was used to calculate a low-
194 expression threshold. A threshold of 10 reads per transcript in this library defined the threshold for
195 transcript retention (count-per-million > 1.19), as suggested in the edgeR documentation. Any transcript
196 passing this threshold in at least five individuals was retained through the first filtering step for initial data
197 visualization and annotation. Additional low expression filtering was conducted in the differential
198 expression analysis and network analysis (see below). Although transcripts were previously annotated in
199 the Phylofish database (Pasquier *et al.* 2016), each transcript was re-annotated using trinotate (Bryant *et*
200 *al.* 2017) and *tblastx* against Swissprot (cutoff = $1e^{-5}$) to obtain as many identifiers as possible for Gene
201 Ontology enrichment analysis. For individual gene descriptions, the re-annotated Swissprot identifier was
202 used primarily, and the Phylofish annotation secondarily.

203

204 *Differential expression analysis between sexes*

205 To reduce the number of transcripts with very low expression in the differential expression analysis, we
206 applied a low expression filter of cpm > 1.19 in at least 65% of the individuals from each sex (i.e. ≥ 31 /
207 47 females or 35 / 53 males). The data was then normalized using the weighted trimmed mean of M-
208 values (TMM; Robinson and Oshlack 2010) to generate normalized \log_2 expression levels. Using
209 *model.matrix* from edgeR with sex as the data grouping, a genewise negative binomial generalized linear
210 model (*glmFit*) was fit to each gene. Genes with false discovery rate of ≤ 0.05 and linear fold-change \geq
211 1.5 were defined as differentially expressed. These genes were binned into low sex bias (i.e. $1.5 \leq FC \leq 4$)
212 or high sex bias (i.e. $FC > 4$) for each sex (negative FC for females, positive for males), as per previous
213 delimitations (Poley *et al.* 2016).

214

215 *Weighted gene co-expression network analysis (WGCNA) in Brook Charr*

216 To best estimate associations between modules and phenotypes of interest, sexes were analyzed
217 separately, and then the preservation of each module was evaluated in the opposite sex (Langfelder *et al.*
218 2011). Due to the independent analysis of each sex, low expression filters (i.e. cpm > 0.5 in at least five
219 individuals) were conducted separately in each sex, then the data normalized as described above. The

220 average library size was 27,896,535 alignments, indicating $\text{cpm} > 0.5$ corresponds to at least 13.95 reads
221 aligning to the transcript for this mean library size. Sex-specific data was used as an input for weighted
222 gene correlation network analysis (WGCNA; Langfelder and Horvath 2008; 2012) in R (R Core Team
223 2018).

224 Within each sex, sample outliers were detected and removed by clustering samples based on
225 transcript expression by Euclidean distance and visually inspecting relationships with the *hclust* average
226 agglomeration method of WGCNA (Langfelder and Horvath 2008). Removal of outliers prevents
227 spurious correlations of modules due to outlier values and improves network generation (Langfelder *et al.*
228 2011). Remaining samples were then correlated with trait data using *plotDendroAndColors*. Network
229 parameters for both female and male networks were defined as per tutorials using unsigned correlation
230 networks (Langfelder and Horvath 2008). Unsigned networks consider the connectivity between identical
231 positive or negative correlations to be equal, and thus genes in the same module may have similar or
232 inverse expression patterns. An optimal soft threshold power (6) was identified by evaluating effects on
233 the scale free topology model fit and mean connectivity by increasing the threshold power by 1 between
234 1-10 and by 2 between 12-20 (Figure S1), as suggested by Langfelder and Horvath (2008). An unsigned
235 adjacency matrix was generated in WGCNA to identify the 25,000 most connected transcripts to retain
236 for reducing computational load. Then, to further minimize noise and spurious associations, adjacency
237 relationships were transformed to the Topological Overlap Matrix using the *TOMdist* function
238 (Langfelder and Horvath 2008).

239 Similarity between modules was evaluated using module eigengenes (i.e. the first principal
240 component of the module). Dissimilarity between eigengenes was calculated by signed Pearson
241 correlation as suggested by Langfelder and Horvath (2008) and plotted using *hclust*. When modules were
242 more than 0.75 correlated (dissimilarity 0.25), they were merged as suggested by Langfelder and Horvath
243 (2008). Merged module eigengenes were then tested for associations with phenotypes by Pearson
244 correlation. Notably the sign of the correlation does not necessarily indicate the direction of the
245 relationship between the expression of specific genes in each module and the phenotype because the
246 modules were built using unsigned networks.

247 Module membership (i.e., the module eigengene-gene correlation) was used to define the top
248 central transcripts for each module (i.e., hub genes). Gene significance (i.e., the absolute value of the trait-
249 gene correlation) was calculated for each transcript against traits weight, specific growth rate, condition
250 factor, hepatosomatic index, change in cortisol, osmolality and chloride from the brief handling stressor,
251 female egg diameter, and male sperm concentration and diameter. Module eigengenes were tested for
252 correlation against traits using Pearson correlation ($p \leq 0.01$).

253 Gene Ontology enrichment analysis of transcripts within each module was conducted using the
254 re-annotated Swissprot identifiers in DAVID Bioinformatics (Huang *et al.* 2009). Heatmaps for modules
255 of interest were generated by using the package *gplots* using the normalized log₂ cpm data (Warnes *et al.*
256 2016). Expression values were standardized across samples for each transcript and Pearson correlation
257 was used to cluster transcripts and samples.

258 To determine sex-specific or sex-conserved modules, module preservation was evaluated by
259 comparing male transcript expression to the generated female modules, and visa-versa, using the
260 *modulePreservation* function of WGCNA. A total of 200 permutations of randomly assigned module
261 labels were used to calculate module preservation rank and Zsummary (Langfelder *et al.* 2011). Low
262 Zsummary scores indicate no preservation (≤ 2), intermediate indicate moderate preservation (2-10) and
263 high scores (≥ 10) indicate strong module preservation (Langfelder *et al.* 2011). The similarity in ranking
264 of modules in terms of preservation in the two different comparative networks (i.e., the opposite sex in
265 Brook Charr and the male Arctic Charr data) was performed by testing the correlation of the module
266 preservation statistic using Spearman rank correlation in R. Module quality was also determined for each
267 module as a measure of module robustness that is characterized by conducting the analysis on multiple
268 random subsets of the original data (Langfelder *et al.* 2011). In addition, cross-tabulation of the
269 proportions of female modules in male modules and visa-versa were performed in R. Cross-tabulation
270 requires similar modular structures of the compared networks, whereas adjacency comparisons directly
271 compare co-expression independent of network topology. All pipelines to analyze the current data are
272 documented and available on GitHub (see *Data Availability*).

273

274 *Module preservation in Arctic Charr*

275 To compare module preservation between Brook Charr and Arctic Charr *S. alpinus* we used RNA-seq
276 data from 1+ year-old Arctic Charr. The broodstock of this population was reared in hatchery conditions
277 for three generations after being collected from a subarctic, land-locked population in Finland (Lake
278 Kuolimo, 61°16' N; 27°32' E). The data were collected from nine male liver samples (fish relatedness not
279 known) from each of 8 °C and 15 °C (total = 18 samples), but due to a large effect of temperature on the
280 transcriptome, and differences between sampling times in the 15 °C group, only the nine samples from the
281 8 °C, group were used here (normal rearing temperature during summer at the fish hatchery; Figure S2)
282 (Prokkola *et al.* 2018). Fish body mass at 8°C was on average 24.2 g ± standard deviation (S.D.) 10.4 g.

283 Sample processing was explained fully by Prokkola et al (2018) and briefly described here. In
284 August 2013, fish were euthanized using 200 ppm sodium bicarbonate-buffered tricaine methanesulfonate
285 (MS-222), after which liver samples were collected and flash frozen in liquid nitrogen (Prokkola *et al.*
286 2018). RNA was extracted from approximately 10 mg of liver tissue using Tri-reagent (Molecular

287 Research Center), and quality checked using a BioAnalyzer (Agilent), with an average identified RNA
288 integrity number of 9.95. Strand-specific cDNA library preparation and sequencing were conducted at
289 Beijing Genomics Institute (BGI Hong Kong) using TruSeq RNA Sample Prep Kit v2 (illumina) and
290 sequenced on an Illumina HiSeq2000 instrument to generate paired-end 100 bp reads. All samples were
291 pooled with unique barcodes across four sequencing lanes. Adapters were removed at BGI, and reads
292 trimmed with Trimmomatic (Bolger et al. 2014) using options *leading* and *trailing* (5) *slidingwindow*
293 (4:15) and *minlen* (36). From samples included in this study, on average $41.7 \pm$ S.D. 7.4 million reads
294 were obtained.

295 Transcript expression was calculated as above, including using the Brook Charr reference
296 transcriptome for ease of cross-species comparisons. Low expression filtering and normalization for the
297 Arctic Charr data was conducted as above (cpm > 0.5 in at least five individuals). However, a network
298 was not constructed for these samples. Using samples from both temperatures, modules were previously
299 identified (Prokkola *et al.* 2018). Once normalized and input to WGCNA, read counts in Arctic Charr 8°C
300 samples were used to build a gene adjacency matrix, which was then compared against modules generated
301 for female and male Brook Charr samples using the *modulePreservation* function as described above.
302 Caveats regarding this data should be noted, including the smaller sample size, immature state of Arctic
303 Charr, minor differences in rearing environments (albeit both were reared in hatchery conditions), and
304 unknown relatedness.

305

306 *Identifying one transcript per gene and assigning chromosome positions*

307 The Brook Charr reference transcriptome (Pasquier *et al.* 2016) possibly contains multiple isoforms for
308 individual genes (Y. Guiguen, *pers. comm.*). Therefore an approach was taken here to reduce multiple
309 genes to a single transcript per gene for enrichment analyses on the sex chromosome or in sex-specific
310 modules. First, the Brook Charr reference transcriptome was aligned to the Atlantic salmon *Salmo salar*
311 chromosome-level genome assembly RefSeq GCF_000233375.1 (Lien *et al.* 2016) using GMAP (Wu and
312 Watanabe 2005). Alignments were converted to an indexed bam retaining only high quality (-q 30)
313 alignments using samtools (Li *et al.* 2009). The indexed bam was converted to a bed file using bedtools
314 *bamtobed* (Quinlan and Hall 2010). Second, the lengths of Brook Charr transcripts were calculated using
315 custom python scripts (see *Data Availability*). With the alignment position, lengths, and expression status
316 (expressed or not expressed), a single transcript per contiguous (or overlapping) alignment block on the
317 reference genome was retained using a custom R script (see *Data Availability*). For each contiguous
318 alignment block, this script preferentially retained the longest, expressed transcript. All other redundant
319 transcripts, and all that did not align, were not retained. In some cases, a single transcript can align to

320 multiple locations with high mapping quality ($\text{MAPQ} \geq 30$). Since there was no reason to retain one
321 alignment over another, both alignments were retained in the baseline set for these cases.

322 The alignment information per retained Brook Charr transcript was used to assign an Atlantic
323 Salmon chromosome identifier to each retained unique transcript. The chromosome information was
324 combined with the module information for all transcripts in each sex-specific network. This analysis was
325 conducted separately for females and males, as expressed genes were in some cases different between the
326 two sexes and therefore so would be the selection of which transcript to retain. The correspondence
327 between the Atlantic Salmon genome assembly accession identifier and the Atlantic Salmon chromosome
328 identifier were obtained from the NCBI genome assembly website (see *Data Availability*). In general,
329 correspondence of gene synteny is expected to be similar between Atlantic Salmon and Brook Charr
330 (Sutherland *et al.* 2016). Using the chromosome correspondence table in Sutherland *et al.* (2016), the
331 Atlantic Salmon chromosome containing the sex chromosome of Brook Charr was identified. For each
332 sex-specific co-expression module, the proportions of Brook Charr genes located on the Atlantic Salmon
333 chromosome that corresponds to the Brook Charr sex chromosome were characterized and compared to
334 the total list of all non-redundant Brook Charr transcripts identified. Fisher exact tests were then used to
335 determine significance for each sex-specific module-sex chromosome combination (i.e., two tests). The
336 chromosome information was also combined with the sex bias fold change values. Finally, the proportion
337 of highly or moderately sex-biased transcripts for females and males were investigated for
338 overrepresentation on the sex chromosome and in sex-specific or conserved modules using Fisher's exact
339 tests in custom R scripts (see *Data Availability*).

340

341 *Data Availability*

342 Brook Charr raw sequence data is available on SRA under BioProject PRJNA445826, accession
343 SRP136537. The bioinformatics pipeline to analyze this data is available at
344 https://github.com/bensutherland/sfon_wgcna. Additional results that support the main text are available
345 in the Supplemental Results section. Module assignments for transcripts in networks, differential
346 expression results, and gene expression counts are provided in the supplemental information.

347

348 **RESULTS**

349 *Transcriptome overview*

350 Of the total 69,440 transcripts in the Brook Charr reference transcriptome, 51,911 passed initial low
351 expression filters when using all samples together. Low-expression filtering for differential expression
352 analysis (i.e., expressed in at least 65% of individuals from one of two sexes) resulted in the retention of
353 42,622 transcripts. Low-expression filtering for sex-specific network analysis (i.e., expressed in at least

354 five individuals of the sex of interest) resulted in 50,748 and 50,530 transcripts passing filters in females
355 and males, respectively. When considering each sex individually, most of the expressed genes were
356 expressed in a majority of the samples: females expressed 35,461 transcripts in > 90% of the samples;
357 males expressing 35,714 transcripts in > 90% of the samples (Figure S3).

358 Hierarchical clustering of samples by gene expression indicated a large effect of sex, where 35 of
359 47 F₂ females clustered with the F₁ female, and 52 of 53 F₂ males were clustered together with the F₁ male
360 (Figure 1). As described in the Methods, outliers were removed to avoid spurious network correlations
361 (Langfelder *et al.* 2011), and this included the removal of one male leaving 52 males remaining, and the
362 removal of one group of females that had large liver weight, leaving 35 females remaining (see phenotype
363 liver weight in Figure 1; Figure S4). When these outlier samples were included while constructing the
364 female network, many modules correlated with the liver weight phenotype (*data not shown*), suggesting
365 that these samples were having a large impact on the network.

366 Interestingly, females displayed higher inter-individual variance in gene expression than males, as
367 indicated by the multiple smaller sample clusters of females in the hierarchical clustering relative to the
368 fewer and larger sample clusters of the males (Figure 1). Likewise, six of the phenotypic traits also
369 displayed higher variance in females (significant heteroscedasticity at $P < 0.05$, Levene's test): liver
370 weight, cortisol level, osmolality, and change in cortisol, osmolality and chloride levels due to handling
371 (Figure S5). Some of the higher variance in these traits in females was likely explained by maturity, but
372 maturity did not explain all of the variance within the female gene expression, as the different sample
373 clusters observed had a variety of maturity states, and samples that were all determined to be mature were
374 present in different sample clusters (Figure 1). In the following, the sex-specific networks will be
375 presented and compared against the alternate sex and the congener Arctic Charr.

376

377 *Network construction and phenotype correlations: female Brook Charr*

378 Highly correlated module eigengenes ($r > 0.75$) were merged, combining 81 modules into 14 (Figure
379 S6A; Figure S7A). Assigned female modules each contained a range of 77-10,533 transcripts (Table 1).
380 The largest module was *darkred*, with 10,533 transcripts (see Table 1), which included more transcripts
381 than even the unassigned *grey* module (second largest; 5,892 transcripts).

382 Correlations of module eigengenes with specific phenotypes ($n = 15$) indicate potential functional
383 associations of the modules (Table 1; Figure 2). The strongest associations of phenotypes to modules
384 were with maturity index, for example with *thistle2* ($r > 0.81$), and *corall* ($r = -0.83$). Although the large
385 liver weight outlier samples were removed prior to network generation, liver weight remained highly
386 correlated with *indianred4* ($r = 0.73$), *salmon*, *coral* ($r = 0.52$), and *blue2* ($r = -0.64$). Growth rate showed
387 similar module correlations to liver weight (Figure 2). Osmolality change was also correlated with

388 *indianred4* ($r = 0.56$) and *blue2* ($r = -0.58$), as well as with *darkred*, *thistle3* ($r \geq 0.51$), *darkorange*, *green*
389 and *darkmagenta* ($r \geq |-0.49|$). Chloride change had no significant associations, but post-stress chloride
390 was correlated with *thistle3* ($r = 0.56$) and *lightsteelblue* ($r = -0.53$). Although no modules were
391 significantly associated with cortisol (change or post-stress; $p \geq 0.01$), *ivory* was close ($r = -0.38$; $p =$
392 0.03).

393 In order to understand the gene composition of modules, Gene Ontology functional enrichment
394 analysis of the transcripts within each module was conducted (Table 1; Additional File S1). The *salmon*
395 module (correlated with liver weight) was enriched for erythrocyte development. The *blue2* module (liver
396 weight) was associated with ribonucleoprotein complex. *Darkorange*, *green*, and *darkmagenta* modules
397 (all correlated with osmolality change) were enriched for small molecular metabolic process, translation
398 and metabolism functions, respectively. One module did not have significant enrichment of biological
399 processes, *lightsteelblue* (correlated with chloride change).

400

401 *Preservation of co-expression: female Brook Charr network*

402 The preservation of co-expression of female Brook Charr modules in Brook Charr males was primarily
403 evaluated using network adjacency comparisons, which are more sensitive and robust than cross-
404 tabulation methods (Langfelder *et al.* 2011). Most female modules were preserved in males and only
405 *darkred* had weak evidence for preservation (Table 1). *Green* was the most conserved ($Z_{\text{summary}} = 100$),
406 followed by *blue2*, *salmon*, *lightsteelblue* and *darkorange* ($Z_{\text{summary}} \geq 48$; Table 1). Modules associated
407 with translation activities were among the highest conserved modules (e.g. *green* and *blue2*).

408 Published male Arctic Charr liver transcriptome data was then compared to the network to
409 evaluate cross-species module preservation (Prokkola *et al.* 2018). Even with caveats regarding sample
410 size (see Methods), several female Brook Charr modules were highly preserved in Arctic Charr males,
411 including *blue2* ($Z_{\text{summary}} = 34$), *green* ($Z_{\text{summary}} = 24$), and *salmon* ($Z_{\text{summary}} = 17$), also the most
412 conserved in male Brook Charr (Table 1). Other female Brook Charr modules with moderate evidence for
413 preservation in male Arctic Charr included *darkorange* and *lightsteelblue* ($Z_{\text{summary}} > 8$), which were
414 also highly preserved in male Brook Charr. It is noteworthy that the ranking of preservation of female
415 modules in the Arctic Charr and Brook Charr males is highly similar (Table 1; Spearman $\rho = 0.895$; $p <$
416 0.00005 ; Figure S8).

417

418 *Network construction, phenotype correlations, and sex-specificity: male Brook Charr*

419 Highly correlated male modules (eigengene correlation $r > 0.75$) were merged, reducing 44 assigned male
420 modules to 25 (Figure S6B; Figure S7B). Unlike the female network, a large proportion of the male data
421 could not be assigned to a module. The unassigned *grey* module contained 72% of the analyzed

422 transcripts (17,992 transcripts). Assigned modules each contained between 54-1,732 transcripts (Table 2;
423 Additional File S2). Phenotypic correlations with male module eigengenes were tested (Figure S9; see
424 Supplemental Results; summarized in Table 2). Of note were several modules enriched for immunity-
425 related functions, including *darkmagenta* (defense response to virus) and *steelblue* (positive regulation of
426 innate immune response) (Table 2 and Additional File S1). These two immune processes were found to
427 belong to different modules that were not just inversely regulated but rather having somewhat decoupled
428 regulation, given that the network constructed was unsigned and thus the sign of the correlation does not
429 affect whether the genes are grouped (Figure 3A). However, these modules were still correlated even if
430 not grouped into a single module (Figure S7B).

431 Preservation of male modules in females was also evaluated, but in contrast to what was observed
432 in the preservation of female modules in males (see above), many of the male modules were weakly to
433 moderately preserved in the females. Highly preserved modules included *yellow* ($Z_{\text{summary}} = 58$; Figure
434 3B) and *brown* ($Z_{\text{summary}} = 38$), *tan* ($Z_{\text{summary}} = 43$), and *lightcyan* ($Z_{\text{summary}} = 34$). Some modules
435 were less preserved, and therefore more sex-specific, than even the randomly generated *gold* module
436 (Table 2) and the unassigned *grey* module, including *green* (translation and size; $Z_{\text{summary}} = 4.5$),
437 *darkgrey* (mitochondrial membrane; $Z_{\text{summary}} = 1.8$) and *ivory* (transcription factor activity; Z_{summary}
438 $= 0.8$; Figure 3C). Preserved modules *yellow* and *brown* were enriched for ribosomal or translation-
439 related functions, as was the more sex-specific *green* module (Table 2). *Ivory*, the most sex- and species-
440 specific male module (see below; Table 2; Figure 3C) was enriched for neurogenesis in GO biological
441 process, but also transcription factor activity in GO molecular function (Additional File S1). Other non-
442 preserved or lowly preserved modules were enriched for membrane activity including *darkgrey*
443 (mitochondrial inner membrane) and *lightcyan1* (membrane organization; Additional File S1).
444 Preservation of male Brook Charr modules was also explored in Arctic Charr males. Similar to that
445 observed in the female modules, when a male Brook Charr module was preserved in female Brook Charr,
446 it was also often preserved in male Arctic Charr (Table 2; Spearman $\rho=0.69$; $p < 0.0005$; Figure S8).

447

448 *Sex-biased transcripts, sex-specific modules, and the sex chromosome*

449 To further understand the relation between sex-bias in gene expression and sex-specificity in network
450 architecture, a gene-by-gene differential expression analysis between the sexes was conducted. Of the
451 42,622 expressed transcripts, 6,983 (16.4%) were differentially expressed ($FC \geq 1.5$; $\text{glmFit FDR} \leq 0.05$).
452 Female-biased genes included 3,989 moderately (1.5-4-fold) and 236 highly biased (>4-fold) transcripts.
453 Highly biased transcripts included known sex-biased genes such as *vitellogenin*, and *zona pellucida*
454 *sperm-binding proteins*. Male-biased genes included 2,638 moderately and 120 highly biased transcripts,

455 including *semaphorin-3F* (most highly male-biased transcript). For a complete list, see Additional File
456 S3.

457 Interestingly, sex-biased transcripts were not overrepresented in female or male sex-specific
458 modules (Table 3). However, unexpectedly, highly male-biased genes were overrepresented in highly
459 preserved modules (36 transcripts in highly preserved modules, 97% of the highly sex-biased transcripts)
460 in comparison to the overall percentage in the network (4,886 transcripts in highly preserved modules,
461 76.5% of network transcripts; Table 3; two-sided Fisher's exact test $p = 0.0013$). The female data was
462 more similar between the highly sex-biased transcripts and the entire network (45.2% and 46.6%,
463 respectively). Sex-specific modules were not enriched on the sex chromosome (Fisher's exact test $p >$
464 0.5), including male modules *ivory* and *darkgrey* (Table S1).

465 Of the 47 non-overlapping, highly male-biased transcripts assigned to chromosomes, five were on
466 the sex chromosome (10.6%), relative to 779 on the sex chromosome of the 12,934 expressed in males
467 (Ssa09; 6.0%). However, this difference was not significant (one-sided Fisher's exact test $p = 0.15$).
468 Furthermore, moderately male-biased transcripts were not enriched on the sex chromosome (5.3%)
469 relative to all expressed transcripts (6%), nor were highly or moderately female-biased transcripts (high
470 bias = 4.1%; moderate bias = 5.8%).

471

472 DISCUSSION

473 Gene co-expression produces complex phenotypes and may underlie key aspects of phenotypic evolution
474 (Filteau *et al.* 2013) and sexual dimorphism (Chen *et al.* 2016). One of the main challenges in producing
475 females and males is developing different phenotypes from largely the same set of genes (Rowe *et al.*
476 2018). Transcriptome architecture may provide a solution to this challenge. In this study, co-expression
477 networks for both female and male Brook Charr liver transcriptomes were characterized and compared to
478 each other. Although the female network had much higher module assignment of expressed transcripts, in
479 general most modules were preserved between the sexes. Two sex-specific modules were identified in
480 males that may provide insight on the evolution of gene expression and phenotypic sexual dimorphism.
481 Sex bias was observed in 16% of the expressed transcripts, and surprisingly these sex-biased transcripts
482 were not overrepresented in sex-specific modules. This indicates the value of using these two different
483 approaches given that different information was obtained from each.

484

485 *Sex differences in co-expression networks and cross-species preservation*

486 Females and males clustered distinctly in unsupervised clustering by gene expression, as has been
487 observed in other studies of fish liver at a reproductive stage (Qiao *et al.* 2016). Interestingly, there was a
488 large difference in the number of transcripts assigned to modules between the sexes; of the 25 k most

489 connected transcripts, females had 76% transcripts assigning to a module, and males only 28%.
490 Importantly, this observation coincides with higher inter-individual variation in gene expression in
491 females than in males (Figure 1) and higher inter-individual variation in six phenotypes in females than in
492 males (Figure S5). When inter-individual variation in gene expression is low, transcripts will not be as
493 well clustered, because without variance there can be no co-variance for clustering algorithms to act upon
494 (Tritchler *et al.* 2009). Therefore, the lower variance in male gene expression may have resulted in the
495 observed lower module assignment. The observation of lower variation in phenotypes is an interesting
496 result that highlights similarities between transcriptomic and phenotypic expression. Building networks in
497 both sexes allowed for the identification of this lower assignment to modules in males, which may have
498 not been noted otherwise, as female modules generally were scored as preserved in males. Furthermore,
499 this allowed the identification of many male network modules with seemingly important and different
500 functional associations that in the female network were all grouped together into one very large module
501 (i.e., *darkred*). The reason for the grouping of these multiple male modules all together into a single
502 female module is not clear, but could be due to an increased effect of maturity on the data in females that
503 may be swamping out the other more subtle covariances in the data. This further indicates the value of
504 doing separate analyses in each sex, in order to avoid signal being overwhelmed by phenotypes that
505 impact the data more in one sex than the other. It will be valuable to inspect sex-specific module
506 generation in other salmonids and in tissues other than liver to understand the generality of these sex
507 differences and associations to inter-individual variance in gene expression and phenotypes.

508 Our observations confirm previous findings that co-expression patterns are often preserved
509 between sexes or closely related species (van Nas *et al.* 2009; Wong *et al.* 2014; Cheviron and Swanson
510 2017). Here, highly preserved modules between the sexes were often comprised of genes within pathways
511 involved in conserved functions. The most preserved modules between the sexes and species were
512 involved in basic cellular processes and included many co-expressed subunits of a multiple subunit
513 protein complex, such as translation machinery. Multiple subunits and functionally related genes have
514 long been known to cluster together by co-expression (Eisen *et al.* 1998). Immunity-related modules were
515 also preserved between the sexes, with co-expression patterns similar to those observed previously in
516 salmonids (Sutherland, *et al.* 2014b). Considering the importance of immune function to both sexes, it is
517 not surprising that immunity modules are preserved between sexes.

518 The male-specific module *darkgrey* and the lowly preserved *green* module were both associated
519 with size, which can be sexually dimorphic in salmonids and is associated to breeding success in males
520 (Blanchfield *et al.* 2003). In comparison, no female modules were associated to length and weight, further
521 suggesting that these more male-specific modules could have a role in producing a sexually dimorphic
522 phenotype. The other male-specific module, *ivory*, may contribute to sexual dimorphism and resolution of

523 sexual antagonism by being an upstream controller of different programs, as it is enriched for
524 transcription factor activity and hub genes as putative transcription factors. Hub genes of *ivory* include
525 genes from the *wnt* protein family. Wnt signaling is associated with gonad differentiation and shows sex-
526 specific expression in several studies in mammals and fish (Vainio *et al.* 1999; Nicol and Guiguen 2011;
527 Sreenivasan *et al.* 2014; Böhne *et al.* 2014). Future studies could investigate whether transcription factors
528 from the sex-specific *ivory* module control expression of transcripts found to be sex-biased here once
529 transcription factor binding sites are characterized in this species.

530 The presence of sex-specific modules and sexually dimorphic gene expression in the liver
531 corresponds with what is known about sex hormones produced in the gonads, as these hormones have
532 been shown to regulate a significant proportion of the liver transcriptome in mouse (van Nas *et al.* 2009).
533 In a large-scale transcriptome study in humans, the liver was not one of the most sexually dimorphic in
534 terms of sex-biased genes (Chen *et al.* 2016). In oviparous species at a reproductive stage however, this
535 tissue is highly sexually dimorphic, given the role in females for producing oocyte constituents (e.g.
536 *vitellogenins*, *zona pellucida* proteins) (Qiao *et al.* 2016). Some of the strongest phenotypic associations
537 of female modules were to maturity. These associations may reflect the effects of sex hormones such as
538 estradiol, which controls reproduction and has a strong influence on transcription in fish (Garcia-Reyero
539 *et al.* 2018). There were no male modules associated to maturity, but there were only six females and two
540 males retained in the analysis that were immature, which prevents a comparison of maturation-related
541 transcripts between the sexes.

542 The ranking of module preservation levels in both the opposite sex and in Arctic Charr was often
543 similar, suggesting evolutionary conservation for many gene co-expression modules. Even with the lower
544 sample size in Arctic Charr, moderate and high preservation was identified for eight and three of the
545 female modules ($n = 14$), respectively, and for seven and 14 of the male modules ($n = 25$), respectively.
546 Modules preserved across species with significant phenotypic correlations may be worthwhile to
547 investigate further regarding their contribution to phenotypes such as growth rate, reproduction, stress
548 response, and immunity. For example, the preserved module in the male network, *turquoise*, was enriched
549 for immunity and marginally associated with growth ($p = 0.05$), phenotypes known to trade-off
550 (Lochmiller and Deerenberg 2000; van der Most *et al.* 2010).

551 Many sex-biased transcripts were identified ($n = 6,983$ transcripts), but only 154 transcripts were
552 found in sex-specific modules identified through the network comparison approach. Sex-biased
553 expression and sex-specific networks are not always overlapping phenomena (Chen *et al.* 2016). This
554 highlights the large differences between these approaches, but in general they together provided a more
555 comprehensive result than either in isolation. The sex bias analysis found that neither male-biased nor
556 female biased genes were significantly overrepresented on the sex chromosome, but power to detect this

557 may have been reduced by the use of a reference genome of a related species rather than the target
558 species. In other species, male-biased transcripts are more often associated with migration to the sex
559 chromosome (Rowe *et al.* 2018), and although there was a trend towards this for the highly male-biased
560 transcripts here, it was not significant. The relationship of sex chromosomes, sex-biased gene expression
561 and sexual dimorphism is not yet well established (Dean and Mank 2014), and this study is an example of
562 integrating these multiple aspects for improved understanding of the role of transcriptomics in generating
563 sex differences.

564

565 *Case study: modules separated by immune response type*

566 To demonstrate the utility of this network approach in investigating specific phenotypes, the following is
567 an analysis of modules associated with immunity in the male network. Separate modules were identified
568 for immune functions involving innate antiviral genes (i.e., male *darkmagenta*) and innate immunity C-
569 type lectins (i.e., male *steelblue*). This is of large interest considering that these types of immune
570 responses have been observed to respond inversely, where pathogen recognition receptors (e.g. C-type
571 lectins) are up-regulated and innate antiviral genes down-regulated in the anterior kidney during
572 ectoparasite infection (Sutherland *et al.* 2014b) and pathogen recognition receptors are up-regulated and
573 innate antiviral genes are down-regulated in gill tissue during out-migration of steelhead trout
574 *Oncorhynchus mykiss* smolts (Sutherland *et al.* 2014a). Even if the genes are not the same between these
575 studies and ours (i.e., no 1:1 association of orthologs has been done for these datasets), the observation of
576 similar functions in two different modules in the present study may indicate that these functions are
577 hardwired into different modules given that no known infection is occurring within these samples. It is
578 important to note that here unsigned networks were used, and therefore if the two immune response types
579 were completely inversely regulated, they would belong to the same module, which was not observed
580 here. These two modules may therefore not be completely under the same regulatory control as they are
581 not completely inversely correlated. This is a new observation in the regulation of these different immune
582 system processes in salmonids. This is an important avenue for further study given the relevance of these
583 genes to immune responses against pathogens, and the potential response outcomes of co-infection
584 occurring between parasitic and viral agents in nature.

585 The immune response modules observed here (i.e., male *darkmagenta*, *steelblue*, and *turquoise*)
586 were all considered as highly preserved between the sexes and moderately to highly conserved in Arctic
587 Charr. It will be valuable to see if these three modules or the genes within them have conserved
588 expression patterns in other species as these may have important roles in defense responses. The tissue
589 was in a post-stress state, which could affect the induction of immune responses, and so additional
590 observations, such as in a resting state, will be valuable. It is possible that the co-expression viewed in

591 these (and other) modules comes from the occurrence of a specific cell type that is present in different
592 levels in the sampled tissue in different individuals. Single-cell RNA-sequencing of immune cells, or *in*
593 *situ* gene expression hybridization techniques could address some of these questions. Further, to better
594 understand the immunity related modules, it may also be valuable to use a microbe profiling platform
595 alongside transcriptome studies of wild sampled individuals to best understand co-infection details (e.g.
596 Miller *et al.* 2016). Nonetheless, the characterization of salmonid co-expression modules will be
597 strengthened when additional analyses are conducted with a broader range of species, once orthologs are
598 identified among the species.

599

600 *Future comparative approaches and salmonid transcriptome network evolution*

601 When similar datasets are produced in other salmonids, it will be valuable to identify whether the
602 preserved modules are conserved outside of the genus *Salvelinus*. However, importantly this will require
603 identification of 1:1 orthologs among the species, which would enable cross-species analyses. Salmonid
604 ortholog identification across reference transcriptomes has recently been conducted for Atlantic Salmon,
605 Brown Trout *Salmo trutta*, Arctic Charr, and European Whitefish *Coregonus lavaretus* (Carruthers *et al.*
606 2018), as well as Northern Pike (*Esox lucius*), Chinook Salmon (*O. tshawytscha*), Coho Salmon (*O.*
607 *kisutch*), Rainbow Trout (*O. mykiss*), Atlantic Salmon, and Arctic Charr (Christensen *et al.* 2018). This
608 type of approach, combined with non-redundant reference transcriptomes will be invaluable in future
609 studies to enable cross species comparisons.

610 If modules are indeed largely conserved between species, as our study suggests within *Salvelinus*
611 liver, this would indicate that large-scale rewiring of baseline transcription networks has not occurred
612 since the base of the lineage. Species-specific modules will be highly valuable to investigate to better
613 understand transcriptional architecture underlying phenotypic differences between the species. The largest
614 amount of rediploidization is thought to have occurred in the salmonids at the base of the lineage
615 (Kodama *et al.* 2014; Lien *et al.* 2016), although a substantial proportion of ohnologs experienced
616 lineage-specific rediploidization post-speciation events later in evolutionary time (Robertson *et al.* 2017).
617 Given the large potential impact that divergence in regulatory regions or epigenetic signatures can have
618 on gene expression, one could expect large lineage-specific changes in co-expression networks. The
619 impact of the genome duplication and rediploidization on transcriptome networks, including lineage
620 specific changes are important avenues for future study.

621

622

622 **CONCLUSIONS**

623 Co-expression networks and sex-biased expression of female and male Brook Charr liver in a
624 reproductive season shortly after an acute handling stressor were characterized in the present study.

625 Results support previous observations of moderate to high preservation of modules between sexes and
626 closely related species. Highly preserved modules were involved in basic cellular functions and immune
627 functions. Sex-specific modules identified only in the male network were enriched for transcription factor
628 activities and associated with sex-biased or potentially sexually antagonistic phenotypes, such as body
629 size. Higher assignment of transcripts to modules was identified in the female network, potentially due to
630 higher inter-individual variance in gene expression and phenotypes. Important physiological functions
631 such as immunity response types were captured by this analysis, identifying not only inverse regulation
632 between two immunity responses but potentially decoupled regulation, which has implications for
633 responses to co-infections and requires further study. This dataset has provided new insights into the
634 transcriptome network structure differences between sexes and has pointed towards individual genes and
635 gene modules that may be involved with generating sexually dimorphic phenotypes and potentially
636 alleviating sexually antagonistic selection.

637

638

ACKNOWLEDGEMENTS

639 Thanks to Guillaume Côté for laboratory assistance, Jérémy Le Luyer and Marie Filteau for discussions
640 about WGCNA, Eric Normandeau for discussion on gene annotation, Yann Guiguen for discussion on
641 details of transcriptome assembly, Phineas Hamilton for statistical discussion, and Aimee-Lee Houde,
642 three anonymous reviewers and the Editors for comments on the manuscript. This work was funded by a
643 Fonds de Recherche du Québec (FRQ) Nature et Technologies research grant awarded to Céline Audet,
644 Louis Bernatchez, and Nadia Aubin-Horth; a grant from the Société de Recherche et de Développement
645 en Aquaculture Continentale (SORDAC) awarded to L.B. and C.A. J.M.P. is supported by the Finnish
646 Cultural Foundation. During this work, B.J.G.S. was supported first by a Natural Sciences and
647 Engineering Research Council of Canada postdoctoral fellowship and subsequently by an FRQ Santé
648 postdoctoral fellowship.

649

650

REFERENCES

- 651 Allendorf, F. W., and G. H. Thorgaard, 1984 Tetraploidy and the evolution of salmonid fishes, pp. 1–53
652 in *Evolutionary genetics of fishes*, edited by B. J. Turner. Plenum Publishing Corporation, New York.
- 653 Barson, N. J., T. Aykanat, K. Hindar, M. Baranski, G. H. Bolstad *et al.*, 2015 Sex-dependent dominance
654 at a single locus maintains variation in age at maturity in salmon. *Nature* 528: 405–408.
- 655 Blackmon, H., and Y. Brandvain, 2017 Long-term fragility of Y chromosomes is dominated by short-
656 term resolution of sexual antagonism. *Genetics* genetics.300382.2017–9.
- 657 Blanchfield, P. J., M. S. Ridgway, and C. C. Wilson, 2003 Breeding success of male brook trout
658 (*Salvelinus fontinalis*) in the wild. *Mol. Ecol.* 12: 2417–2428.
- 659 Bolger, A. M., M. Lohse, and B. Usadel, 2014 Trimmomatic: a flexible trimmer for Illumina sequence
660 data. *Bioinformatics* 30: 2114–2120.
- 661 Boula, D., V. Castric, L. Bernatchez, and C. Audet, 2002 Physiological, endocrine, and genetic bases of
662 anadromy in the Brook Charr, *Salvelinus fontinalis*, of the Laval River (Québec, Canada). *Environ*
663 *Biol Fish* 22: 229–242.
- 664 Böhne, A., T. Sengstag, and W. Salzburger, 2014 Comparative transcriptomics in East African Cichlids
665 reveals sex- and species-specific expression and new candidates for sex differentiation in fishes.
666 *Genome Biology and Evolution* 6: 2567–2585.
- 667 Bryant, D. M., K. Johnson, T. DiTommaso, T. Tickle, M. B. Couger *et al.*, 2017 A tissue-mapped Axolotl
668 *de novo* transcriptome enables identification of limb regeneration factors. *Cell Reports* 18: 762–776.
- 669 Bush, W. S., and J. H. Moore, 2012 Chapter 11: Genome-Wide Association Studies. *PLoS Comput Biol*
670 8: e1002822.
- 671 Carruthers, M., A. A. Yurchenko, J. J. Augley, C. E. Adams, P. Herzyk *et al.*, 2018 *De novo*
672 transcriptome assembly, annotation and comparison of four ecological and evolutionary model
673 salmonid fish species. *BMC Genomics* 19: 32.
- 674 Chen, C.-Y., C. M. Lopes-Ramos, M. L. Kuijjer, J. N. Paulson, A. R. Sonawane *et al.*, 2016 Sexual
675 dimorphism in gene expression and regulatory networks across human tissues. *bioRxiv* 1–34.
- 676 Cheviron, Z. A., and D. L. Swanson, 2017 Comparative transcriptomics of seasonal phenotypic flexibility
677 in two North American songbirds. *Integr. Comp. Biol.* 57: 1040–1054.
- 678 Christensen K. A., Rondeau E. B., Minkley D. R., Leong J. S., Nugent C. M., Danzmann R. G., Ferguson
679 M. M., Stadnik A., Devlin R. H., Muzzerall R., Edwards M., Davidson W. S., Koop B. F., 2018 The
680 Arctic charr (*Salvelinus alpinus*) genome and transcriptome assembly. *PLoS ONE* 13: e0204076–30.
- 681 Crête-Lafrenière, A., L. K. Weir, and L. Bernatchez, 2012 Framing the Salmonidae family phylogenetic
682 portrait: a more complete picture from increased taxon sampling. *PLoS ONE* 7: e46662.
- 683 Dean, R., and J. E. Mank, 2014 The role of sex chromosomes in sexual dimorphism: discordance between
684 molecular and phenotypic data. *Journal of Evolutionary Biology* 27: 1443–1453.
- 685 Eisen, M. B., P. T. Spellman, P. O. Brown, and D. Botstein, 1998 Cluster analysis and display of genome-

- 686 wide expression patterns. *Proceedings of the National Academy of Sciences* 95: 14863–14868.
- 687 Ellegren, H., and J. Parsch, 2007 The evolution of sex-biased genes and sex-biased gene expression. *Nat*
688 *Rev Genet* 8: 689–698.
- 689 Filteau, M., S. A. Pavey, J. St-Cyr, and L. Bernatchez, 2013 Gene coexpression networks reveal key
690 drivers of phenotypic divergence in Lake Whitefish. *Molecular Biology and Evolution* 30: 1384–
691 1396.
- 692 Fleming, I. A., 1998 Pattern and variability in the breeding system of Atlantic salmon (*Salmo salar*), with
693 comparisons to other salmonids. *Can. J. Fish. Aquat. Sci.* 55: 59–76.
- 694 Gaiteri, C., Y. Ding, B. French, G. C. Tseng, and E. Sibille, 2014 Beyond modules and hubs: the potential
695 of gene coexpression networks for investigating molecular mechanisms of complex brain disorders.
696 *Genes Brain Behav.* 13: 13–24.
- 697 Garcia-Reyero, N., B. S. Jayasinghe, K. J. Kroll, T. Sabo-Attwood, and N. D. Denslow, 2018 Estrogen
698 signaling through both membrane and nuclear receptors in the liver of Fathead Minnow. *General and*
699 *Comparative Endocrinology* 257: 50–66.
- 700 Gillis, J., and P. Pavlidis, 2012 “Guilt by association” is the exception rather than the rule in gene
701 networks. *PLoS Comput Biol* 8: e1002444.
- 702 Guðbrandsson J., S. R. Franzdóttir, B. K. Kristjánsson, E. P. Ahi, V. H. Maier, K. H. Kapralova, S. S.
703 Snorrason, Z. O. Jónsson, A. Pálsson, 2018 Differential gene expression during early development in
704 recently evolved and sympatric Arctic charr morphs. *PeerJ* 6: e4345.
- 705 Horreo, J. L., 2017 Revisiting the mitogenomic phylogeny of Salmoninae: new insights thanks to recent
706 sequencing advances. *PeerJ* 5: e3828–10.
- 707 Huang, D. W., B. T. Sherman, and R. A. Lempicki, 2009 Systematic and integrative analysis of large
708 gene lists using DAVID bioinformatics resources. *Nat Protoc* 4: 44–57.
- 709 Kodama, M., M. S. O. Briec, R. H. Devlin, J. J. Hard, and K. A. Naish, 2014 Comparative mapping
710 between Coho Salmon (*Oncorhynchus kisutch*) and three other salmonids suggests a role for
711 chromosomal rearrangements in the retention of duplicated regions following a whole genome
712 duplication event. *G3 - Genes|Genomes|Genetics* 4: 1717–1730.
- 713 Langfelder, P., and S. Horvath, 2012 Fast R functions for robust correlations and hierarchical clustering.
714 *J. Stat. Soft.* 46: 1–17.
- 715 Langfelder, P., and S. Horvath, 2008 WGCNA: an R package for weighted correlation network analysis.
716 *BMC Bioinformatics* 9: 559.
- 717 Langfelder, P., R. Luo, M. C. Oldham, and S. Horvath, 2011 Is my network module preserved and
718 reproducible? *PLoS Comput Biol* 7: e1001057.
- 719 Langmead, B., and S. L. Salzberg, 2012 Fast gapped-read alignment with Bowtie 2. *Nat Meth* 9: 357–
720 359.
- 721 Li, H., B. Handsaker, A. Wysoker, T. Fennell, J. Ruan *et al.*, 2009 The Sequence Alignment/Map format

- 722 and SAMtools. *Bioinformatics* 25: 2078–2079.
- 723 Lien, S., B. F. Koop, S. R. Sandve, J. R. Miller, M. P. Kent *et al.*, 2016 The Atlantic Salmon genome
724 provides insights into rediploidization. *Nature* 533: 200–205.
- 725 Lochmiller, R. L., and C. Deerenberg, 2000 Trade-offs in evolutionary immunology: just what is the cost
726 of immunity? *Oikos* 88: 87–98.
- 727 Mackay T. F., 2001 The genetic architecture of quantitative traits. *Annu. Rev. Genet.* 35: 303–339.
- 728 Mackay T. F. C., Stone E. A., Ayroles J. F., 2009 The genetics of quantitative traits: challenges and
729 prospects. *Nat Rev Genet* 10: 565–577.
- 730 MacManes, M. D., 2014 On the optimal trimming of high-throughput mRNA sequence data. *Front.*
731 *Genet.* 5: 13.
- 732 Macqueen, D. J., and I. A. Johnston, 2014 A well-constrained estimate for the timing of the salmonid
733 whole genome duplication reveals major decoupling from species diversification. *Proceedings of the*
734 *Royal Society B: Biological Sciences* 281: 20132881–20132881.
- 735 Mähler, N., J. Wang, B. K. Terebieniec, P. K. Ingvarsson, N. R. Street *et al.*, 2017 Gene co-expression
736 network connectivity is an important determinant of selective constraint. *PLoS Genet* 13: e1006402.
- 737 Miller, K. M., I. A. Gardner, R. Vanderstichel, T. Burnley, S. Li *et al.*, 2016 Report on the performance
738 evaluation of the Fluidigm BioMark platform for high-throughput microbe monitoring in salmon., 1–
739 293 p.
- 740 Mueller, A. J., E. G. Canty-Laird, P. D. Clegg, and S. R. Tew, 2017 Cross-species gene modules emerge
741 from a systems biology approach to osteoarthritis. *NPJ Syst Biol Appl* 3: 13.
- 742 Nicol, B., and Y. Guiguen, 2011 Expression profiling of wnt signaling genes during gonadal
743 differentiation and gametogenesis in Rainbow Trout. *Sex Dev* 5: 318–329.
- 744 Oldham, M. C., S. Horvath, and D. H. Geschwind, 2006 Conservation and evolution of gene coexpression
745 networks in human and chimpanzee brains. *Proceedings of the National Academy of Sciences* 103:
746 17973–17978.
- 747 Parsch, J., and H. Ellegren, 2013 The evolutionary causes and consequences of sex-biased gene
748 expression. *Nature Publishing Group* 14: 83–87.
- 749 Pasquier, J., C. Cabau, T. Nguyen, E. Jouanno, D. Severac *et al.*, 2016 Gene evolution and gene
750 expression after whole genome duplication in fish: the PhyloFish database. *BMC Genomics* 17: 368.
- 751 Poley, J. D., B. J. G. Sutherland, S. R. M. Jones, B. F. Koop, and M. D. Fast, 2016 Sex-biased gene
752 expression and sequence conservation in Atlantic and Pacific salmon lice (*Lepeophtheirus salmonis*).
753 *BMC Genomics* 17: 483.
- 754 Prokkola, J. M., M. Nikinmaa, M. Lewis, K. Anttila, M. Kanerva *et al.*, 2018 Cold temperature represses
755 daily rhythms in the liver transcriptome of a stenothermal teleost under decreasing day length. *J. Exp.*
756 *Biol.* 221: jeb170670.
- 757 Qiao, Q., S. Le Manach, B. Sotton, H. Huet, E. Duvernois-Berthet *et al.*, 2016 Deep sexual dimorphism in

- 758 adult medaka fish liver highlighted by multi-omic approach. *Sci. Rep.* 6: 32459.
- 759 Quinlan, A. R., and I. M. Hall, 2010 BEDTools: a flexible suite of utilities for comparing genomic
760 features. *Bioinformatics* 26: 841–842.
- 761 Quinn, T. P., and C. J. Foote, 1994 The effects of body size and sexual dimorphism on the reproductive
762 behavior of sockeye salmon, *Oncorhynchus nerka*. *Animal Behaviour* 48: 751–761.
- 763 R Core Team, 2018 R: A language and environment for statistical computing. R Foundation for Statistical
764 Computing.
- 765 Roberts, A., and L. Pachter, 2013 Streaming fragment assignment for real-time analysis of sequencing
766 experiments. *Nat Meth* 10: 71–73.
- 767 Robertson, F. M., M. K. Gundappa, F. Grammes, T. R. Hvidsten, A. K. Redmond *et al.*, 2017 Lineage-
768 specific rediploidization is a mechanism to explain time-lags between genome duplication and
769 evolutionary diversification. *Genome Biol.* 18: 111.
- 770 Robinson, M. D., and A. Oshlack, 2010 A scaling normalization method for differential expression
771 analysis of RNA-seq data. *Genome Biol.* 11: R25.
- 772 Robinson, M. D., D. J. McCarthy, and G. K. Smyth, 2010 edgeR: a Bioconductor package for differential
773 expression analysis of digital gene expression data. *Bioinformatics* 26: 139–140.
- 774 Rose, N. H., F. O. Seneca, and S. R. Palumbi, 2015 Gene networks in the wild: identifying transcriptional
775 modules that mediate coral resistance to experimental heat stress. *Genome Biology and Evolution* 8:
776 243–252.
- 777 Rowe, L., S. F. Chenoweth, and A. F. Agrawal, 2018 The Genomics of Sexual Conflict. *The American*
778 *Naturalist* 192: 274–286.
- 779 Sauvage, C., M. Vagner, N. Derôme, C. Audet, and L. Bernatchez, 2012a Coding gene single nucleotide
780 polymorphism mapping and quantitative trait loci detection for physiological reproductive traits in
781 Brook Charr, *Salvelinus fontinalis*. *G3 - Genes|Genomes|Genetics* 2: 379–392.
- 782 Sauvage, C., M. Vagner, N. Derôme, C. Audet, and L. Bernatchez, 2012b Coding gene SNP mapping
783 reveals QTL linked to growth and stress response in Brook Charr (*Salvelinus fontinalis*). *G3 -*
784 *Genes|Genomes|Genetics* 2: 707–720.
- 785 Sreenivasan, R., J. Jiang, X. Wang, R. Bártfai, H. Y. Kwan *et al.*, 2014 Gonad differentiation in Zebrafish
786 is regulated by the canonical wnt signaling pathway. *Biology of Reproduction* 90: e34397–10.
- 787 Sutherland, B. J. G., T. Gosselin, E. Normandeau, M. Lamothe, N. Isabel *et al.*, 2016 Salmonid
788 chromosome evolution as revealed by a novel method for comparing RADseq linkage maps. *Genome*
789 *Biology and Evolution* 8: 3600–3617.
- 790 Sutherland, B. J. G., K. C. Hanson, J. R. Jantzen, B. F. Koop, and C. T. Smith, 2014a Divergent immunity
791 and energetic programs in the gills of migratory and resident *Oncorhynchus mykiss*. *Mol. Ecol.* 23:
792 1952–1964.
- 793 Sutherland, B. J. G., K. W. Koczka, M. Yasuike, S. G. Jantzen, R. Yazawa *et al.*, 2014b Comparative

794 transcriptomics of Atlantic *Salmo salar*, Chum *Oncorhynchus keta* and Pink Salmon *O. gorbuscha*
795 during infections with salmon lice *Lepeophtheirus salmonis*. BMC Genomics 15: 200.

796 Sutherland, B. J. G., C. Rico, C. Audet, and L. Bernatchez, 2017 Sex chromosome evolution,
797 heterochiasmy, and physiological QTL in the salmonid Brook Charr *Salvelinus fontinalis*. G3 -
798 Genes|Genomes|Genetics 7: 2749–2762.

799 Thompson, D., A. Regev, and S. Roy, 2015 Comparative analysis of gene regulatory networks: from
800 network reconstruction to evolution. Annu. Rev. Cell Dev. Biol. 31: 399–428.

801 Tritchler, D., E. Parkhomenko, and J. Beyene, 2009 Filtering Genes for Cluster and Network Analysis.
802 BMC Bioinformatics 10: 193–9.

803 Vainio, S., M. Heikkilä, A. Kispert, N. Chin, and A. P. McMahon, 1999 Female development in
804 mammals is regulated by Wnt-4 signalling. Nature 397: 405–409.

805 van Dam, S., U. Vösa, A. van der Graaf, L. Franke, and J. P. de Magalhães, 2017 Gene co-expression
806 analysis for functional classification and gene-disease predictions. Brief Bioinform.

807 van der Most, P. J., B. de Jong, H. K. Parmentier, and S. Verhulst, 2010 Trade-off between growth and
808 immune function: a meta-analysis of selection experiments. Functional Ecology 25: 74–80.

809 van Nas, A., D. Guhathakurta, S. S. Wang, N. Yehya, S. Horvath *et al.*, 2009 Elucidating the role of
810 gonadal hormones in sexually dimorphic gene coexpression networks. Endocrinology 150: 1235–
811 1249.

812 Warnes, G. R., B. Bolker, L. Bonebakker, R. Gentleman, W. Hubert *et al.*, 2016 gplots: Various R
813 Programming Tools for Plotting Data.

814 Wijchers, P. J., and R. J. Festenstein, 2011 Epigenetic regulation of autosomal gene expression by sex
815 chromosomes. Trends Genet. 27: 132–140.

816 Wong, R. Y., M. M. McLeod, and J. Godwin, 2014 Limited sex-biased neural gene expression patterns
817 across strains in Zebrafish (*Danio rerio*). BMC Genomics 15: 905–10.

818 Wright, A. E., M. Fumagalli, C. R. Cooney, N. I. Bloch, F. G. Vieira *et al.*, 2018 Male-biased gene
819 expression resolves sexual conflict through the evolution of sex-specific genetic architecture.
820 Evolution Letters 2: 52–61.

821 Wu, T. D., and C. K. Watanabe, 2005 GMAP: a genomic mapping and alignment program for mRNA and
822 EST sequences. Bioinformatics 21: 1859–1875.

823

824 **TABLES AND FIGURES**

825 **Table 1.** Female modules shown with the number of transcripts within the module (n), the general
826 category of traits correlated with the module ($p \leq 0.01$), the most significantly enriched Gene Ontology
827 category (Biological Process), the Zsummary for preservation of the module in Brook Charr males (BC
828 m) and Arctic Charr males (AC m), as well as the module quality (robustness). Zsummary < 2 is not
829 preserved, $2 < Zsummary < 10$ is moderately preserved, and > 10 is preserved. The *grey* module includes
830 unassigned genes and the *gold* module is a random selection of 1000 genes from the assigned modules for
831 testing preservation metrics. Full module-trait correlations are shown in Figure 2, full GO enrichment in
832 Additional File S1, and expanded summaries of this table in Additional File S2.
833

| Module | n | Traits | GO Enrichment (BP) | Preservation BC m AC m | | Quality |
|-----------------------|-------|---|--|-----------------------------|-------|---------|
| <i>green</i> | 725 | blood | translation | 100 | 24 | 75 |
| <i>blue2</i> | 1762 | blood; liver; maturity; RIN | ribonucleoprotein complex biogenesis | 71 | 32 | 58.5 |
| <i>salmon</i> | 449 | liver; maturity; RIN | erythrocyte development | 56 | 17 | 42 |
| <i>darkorange</i> | 805 | blood | small molecule metabolic process | 48 | 8.8 | 36 |
| <i>lightsteelblue</i> | 77 | blood | <i>none</i> | 48 | 8.2 | 25.5 |
| <i>ivory</i> | 451 | - | ER-associated ubiquitin- dependent protein catabolic process | 37 | 5.4 | 25.5 |
| <i>thistle2</i> | 834 | maturity | tissue development | 29 | 3.6 | 36.5 |
| <i>indianred4</i> | 1180 | blood; growth; liver; maturity; RIN | membrane assembly | 28 | 2.8 | 22 |
| <i>coral1</i> | 689 | liver; maturity; RIN | regulation of cell growth | 25 | 5.2 | 34 |
| <i>thistle3</i> | 235 | blood; liver; size | inorganic anion transmembrane transport | 24 | 1.2 | 21 |
| <i>skyblue1</i> | 96 | RIN | intracellular signal transduction | 17 | 1.2 | 21 |
| <i>darkmagenta</i> | 1072 | blood; maturity | single-organism metabolic process | 13 | 5 | 58 |
| <i>coral2</i> | 200 | - | regulation of blood circulation | 11 | 2.8 | 14 |
| <i>grey</i> | 5892 | Not a module | Not a module | 9 | 2.4 | -18 |
| <i>gold</i> | 1k* | blood; size | Not a module | 4.8 | 0.38 | -0.86 |
| <i>darkred</i> | 10533 | blood | protein ubiquitination | 4.5 | -0.55 | 23.5 |

834

835

836 **Table 2.** Male modules with the number of transcripts within the module (n), the general category of
837 traits correlated with the module ($p \leq 0.01$), the most significantly enriched Gene Ontology category
838 (Biol. Proc.), the Zsummary for preservation of the module in Brook Charr females (BC f) and Arctic
839 Charr males (AC m), as well as the identified module quality (robustness). Zsummary < 2 is not
840 preserved, $2 < Zsummary < 10$ is moderately preserved, and > 10 is preserved. The *grey* module includes
841 unassigned genes and the *gold* module is a random selection of 1000 genes from the assigned modules for
842 testing preservation metrics. Full module-trait correlations are shown in Figure S9, full GO enrichment in
843 Additional File 1, and expanded summaries of this table in Additional File S2.

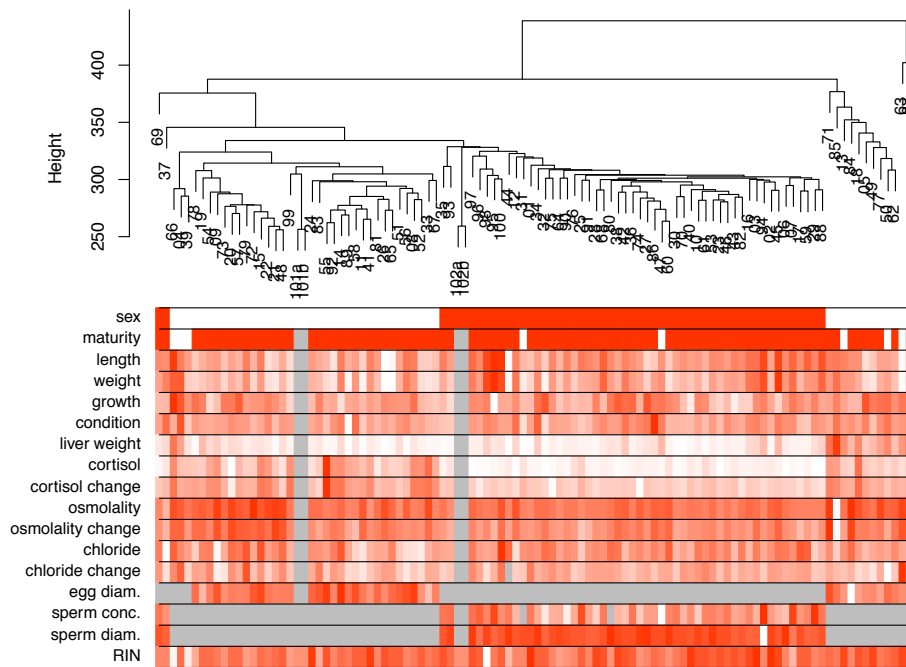
| Module | n | Traits | GO Enrichment (BP) | Preservation | | Quality |
|------------------------|-------|----------------------------------|--|--------------|-------|---------|
| | | | | BC f | AC m | |
| <i>yellow</i> | 339 | blood; liver; size | translation | 58 | 24 | 51 |
| <i>tan</i> | 173 | blood; size | <i>none</i> | 43 | 18 | 41.5 |
| <i>brown</i> | 1732 | blood; sperm | ribonucleoprotein complex biogenesis | 38 | 39 | 72.5 |
| <i>lightcyan</i> | 734 | blood; size | organic acid metabolic process | 34 | 21 | 69 |
| <i>magenta</i> | 226 | <i>none</i> | response to endoplasmic reticulum stress | 32 | 38 | 45 |
| <i>darkmagenta</i> | 61 | <i>none</i> | defense response to virus | 27 | 16 | 25.5 |
| <i>darkgreen</i> | 724 | blood; growth; liver; size | <i>none</i> | 24 | 11 | 58 |
| <i>steelblue</i> | 65 | blood; growth; sperm | positive regulation of innate immune response | 22 | 6.2 | 26.5 |
| <i>violet</i> | 64 | liver | sterol biosynthetic process | 21 | 10 | 29.5 |
| <i>grey60</i> | 147 | <i>none</i> | secretion by cell | 20 | 11 | 39 |
| <i>lightsteelblue1</i> | 55 | <i>none</i> | <i>none</i> | 15 | 0.85 | 23 |
| <i>yellowgreen</i> | 61 | blood | <i>none</i> | 13 | 0.24 | 24.5 |
| <i>turquoise</i> | 783 | <i>none</i> | immune system process | 12 | 14 | 68.5 |
| <i>orangered4</i> | 57 | sperm | regulation of apoptotic process | 12 | 2.3 | 26.5 |
| <i>floralwhite</i> | 52 | <i>none</i> | glutathione metabolic process | 11 | 13 | 25 |
| <i>paleturquoise</i> | 64 | blood | response to organonitrogen compound | 10 | 7.8 | 25.5 |
| <i>lightcyan1</i> | 791 | blood; sperm | cytokinesis | 9.7 | 11 | 67.5 |
| <i>sienna3</i> | 61 | liver; size | extracellular structure organization | 9.6 | 14 | 26.5 |
| <i>plum1</i> | 58 | <i>none</i> | <i>none</i> | 9.6 | 7.4 | 23.5 |
| <i>mediumpurple3</i> | 57 | size | ribonucleoprotein complex assembly | 8.4 | 5.3 | 20.5 |
| <i>darkolivegreen</i> | 138 | blood | <i>none</i> | 7.6 | 11 | 28.5 |
| <i>skyblue</i> | 78 | RIN | regulation of transcription, DNA-templated | 6.7 | 5.8 | 28 |
| <i>grey</i> | 17992 | <i>Not a module</i> | <i>Not a module</i> | 5.5 | 2.3 | -14 |
| <i>gold</i> | 1k* | <i>Not a module</i> | <i>Not a module</i> | 4.9 | 3.2 | -0.035 |
| <i>green</i> | 334 | size | translation | 4.5 | 3.1 | 39 |
| <i>darkgrey</i> | 100 | size | small molecule metabolic process | 1.8 | -0.28 | 31.5 |
| <i>ivory</i> | 54 | blood | neurogenesis | 0.81 | 0.22 | 24 |

844

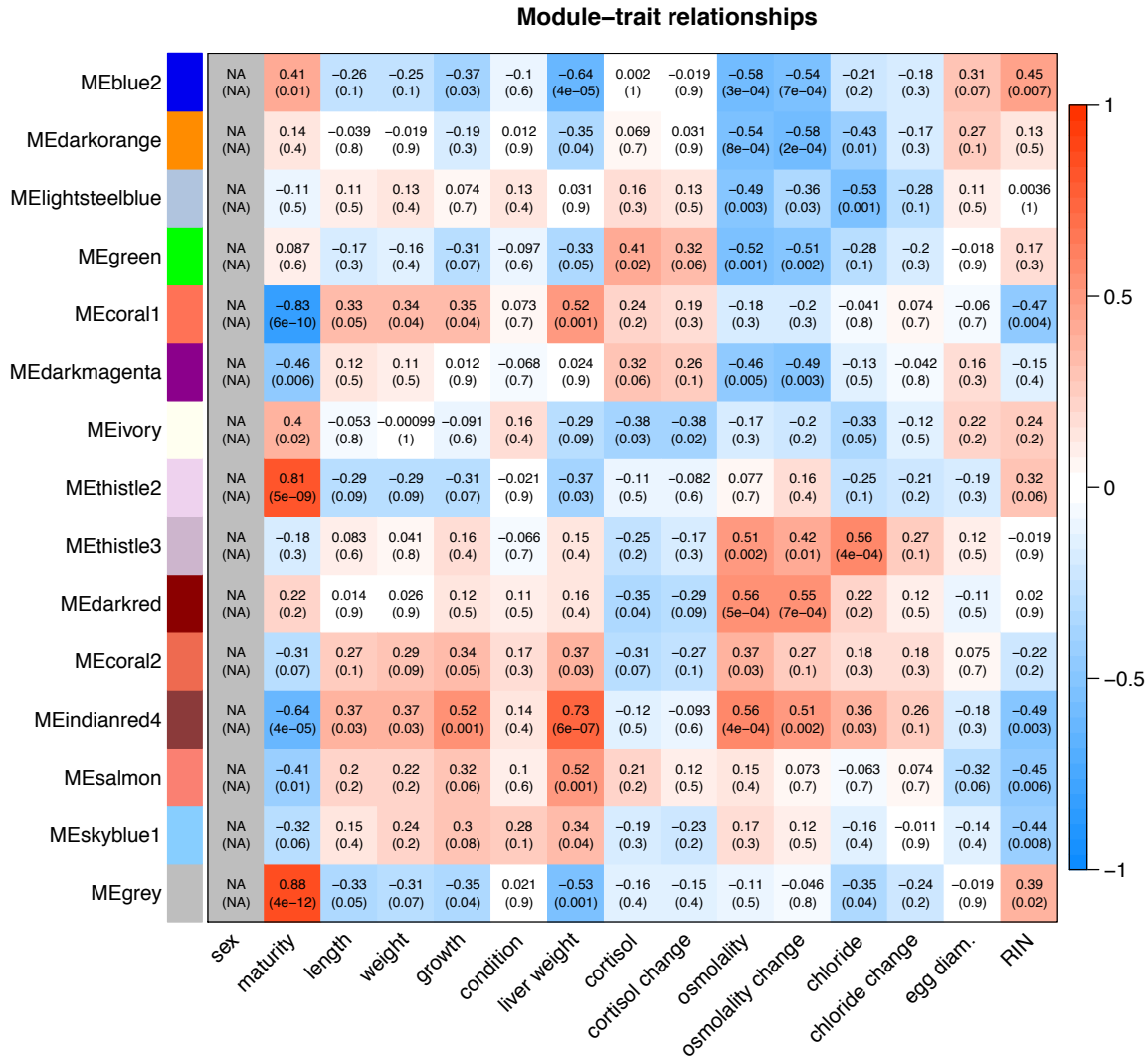
845 **Table 3.** Sex-biased transcript presence in modules that are either unique to each sex (low module
 846 preservation), or moderately or highly preserved, along with the number and percentage of the transcripts
 847 within each sex's sex-biased transcript category (e.g. female high sex-bias). These counts only include
 848 expressed transcripts that are assigned to modules in the network analysis for each sex.
 849

| Sex | Module Preservation in opposite sex | All expressed transcripts count | Moderate sex bias (1.5-4-fold) | High sex bias (>4-fold) |
|---------------|-------------------------------------|---------------------------------|--------------------------------|-------------------------|
| Female | Low | 0 (0%) | 0 (0%) | 0 (0%) |
| | Medium | 9,613 (54.8%) | 744 (52.0%) | 31 (53.4%) |
| | High | 7,929 (45.2%) | 687 (48.0%) | 27 (46.6%) |
| Total | - | 17,542 | 1,431 | 58 |
| Male | Low | 147 (2.3%) | 19 (2.6%) | 0 (0%) |
| | Medium | 1,350 (21.1%) | 119 (16.5%) | 1 (2.7%) |
| | High | 4,886 (76.5%) | 584 (80.9%) | 36 (97.3%) |
| Total | | 6,383 | 722 | 37 |

850
851



852
 853 **Figure 1.** Brook Charr individual samples clustered by gene expression similarity in the liver using all
 854 genes with corresponding quantitative trait values shown in the heatmap below the dendrogram with
 855 intensity of red reflecting the normalized trait value for that sample. Sex was the largest factor affecting
 856 the data (see heatmap sex row; white = females; red = males). Parents were sequenced in duplicate, and
 857 clustered with the offspring of their respective sex (see 101ab for mother and 102ab for father; parents
 858 have grey missing data values for all phenotypes but sex and RIN). Females with large liver weight
 859 clustered outside the other female samples (see on the right-hand side on the liver weight row), and were
 860 removed as they were considered outliers (see Methods).



861

862

863

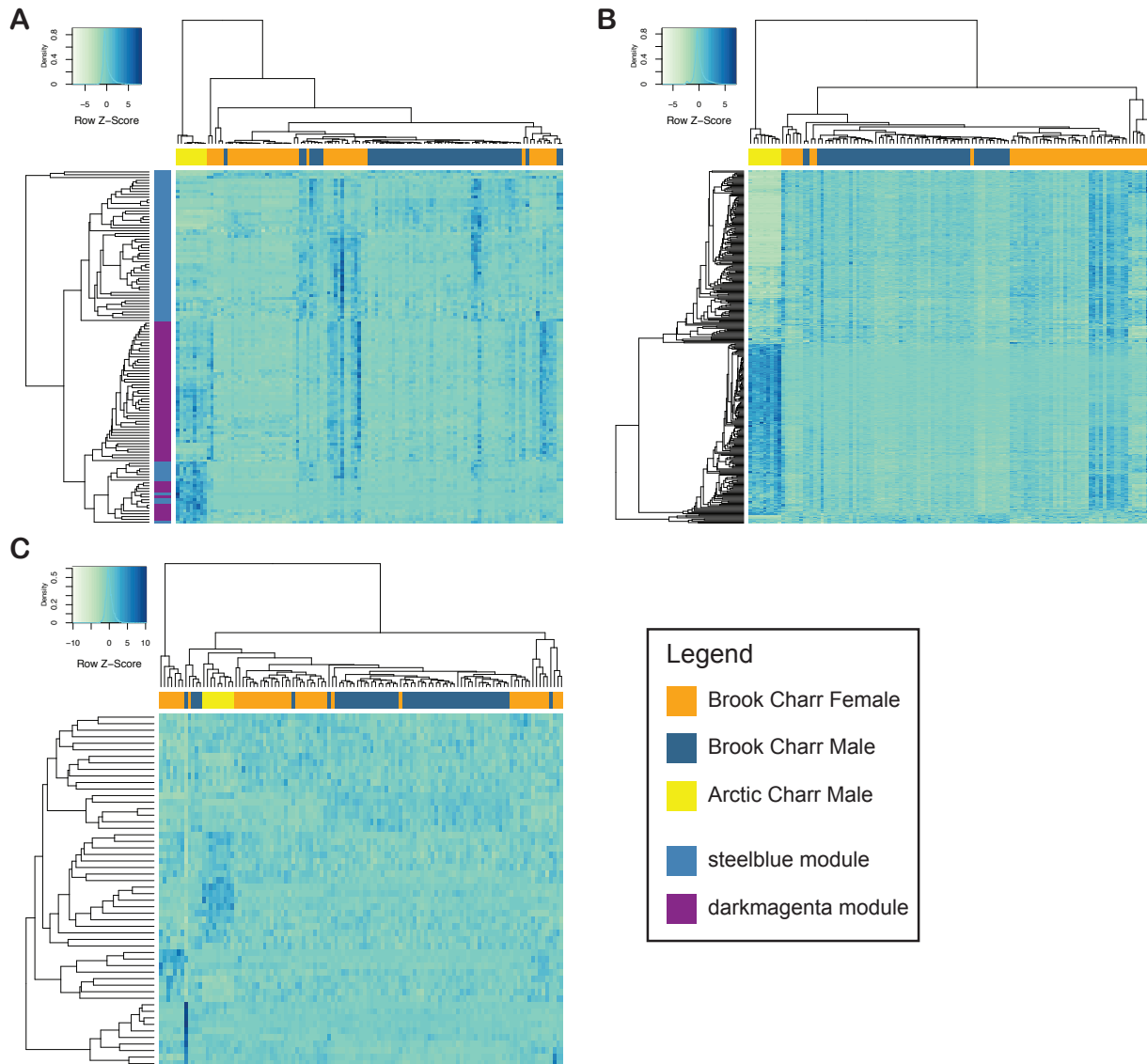
864

865

866

867

Figure 2. Module-trait relationships for Brook Charr females, estimated with Pearson correlation r-values and p-values. The boldness of color indicates the strength of the relationship. Module-trait correlations are also shown in Table 1 with more general grouping of traits alongside other metrics such as module size and enriched Gene Ontology categories. The male network module-trait relationships are shown in Figure S9.



868

869 **Figure 3.** Heatmaps of normalized transcript expression values, clustering both samples and transcripts
 870 using Pearson correlation within (A) two immunity-related male modules, *steelblue* and *darkmagenta*,
 871 which are related to innate immunity and innate antiviral immunity, respectively, (B) the preserved male
 872 module *yellow* (translation), and (C) the male-specific *ivory* (transcription factor activity). Samples are
 873 shown on the horizontal with colors corresponding to the three categories of samples in the legend. The
 874 two modules shown in (A) are colored on the vertical based on the cluster in which the transcript is
 875 contained, as shown in the legend.